ORIGINAL ARTICLE

Desing and evaluation of a sliding bearing for equipment restoration in metallurgical industry

Diseño y evaluación de un cojinete de deslizamiento para recuperación de equipos en la industria minero-metalúrgica

Benigno Leyva-De la Cruz[1], Eli Efraín Guzmán-Romero[1], Marcelo Fabián Salazar-Corrales[2]; Héctor Luis Laurencio-Alfonso[3]; William Giovanny Quitiaquez-Sarzosa[4]; Yoalbys Retirado-Mediaceja[1]*

[1]University of Moa, Holguín, Cuba.

[2]University of the Armed Forces, Latacunga, Ecuador.

[3]Technical University of Cotopaxi, Latacunga, Ecuador.

[4]Salesian Polytechnic University, Quito, Ecuador.

*Corresponding author: yretirado@ismm.edu.cu

Abstract

The study presents the design, manufacture and evaluation of a plain bearing (bushing) intended for the restoration of critical auxiliary equipment used in the nickel mining and metallurgical operations. Reliability and durability of the component was prioritized through a tribological and metallurgical analysis, focusing on the operation regime characterized by radial load of 374,011 N, rotation speed of 2 800 r/min) and service temperature of 60°C. The worn bronze material originally used (CuAl10Ni) was characterized, and phosphorous tin bronze (CuSn14) was selected as a replacement due to its superior hardness (232 HB), ensuring enhanced wear resistance. The design process included clearance and specific load calculations, applying the Sommerfeld number to confirm operation under an elastohydrodynamic (EHL) lubrication regime with ISO VG 460 oil at 60 °C. Manufacturing was carried out on a 16k20 lathe, achieving the required surface roughness with a relative error of 10 %. Technical evaluation indicates that the design guarantees stable EHL lubrication and projects an estimated service life of 1,348,000 hours. This optimized bushing improves the reliability of essential equipment, reducing costly downtime and supporting continuity in key processes of the nickel value chain.

Keywords: tribological analysis, phosphorous bronze, sliding bearing, elastohydrodynamic lubrication

Resumen

El estudio abordó el diseño, fabricación y evaluación de un cojinete de deslizamiento (buje) destinado a la restauración de equipos auxiliares críticos utilizados en las tareas de mantenimiento de la industria minero-metalúrgica del níquel. Se priorizó la fiabilidad y durabilidad del componente mediante un análisis tribológico y metalúrgico, enfocándose en el régimen de operación caracterizado por la carga radial (374,011 N), la velocidad de rotación (2 800 r/min) y la temperatura de servicio (60 ^{0}C). Tras la caracterización del material de bronce desgastado original (CuAl10Ni), se seleccionó el bronce al estaño fosforoso (CuSn14), verificando su dureza superior (232 HB) para garantizar una mayor resistencia al desgaste. El diseño incluyó cálculos de holgura y carga específica, empleando el número de *Sommerfeld* para asegurar la operación bajo un régimen de lubricación elastohidrodinámica (EHL) con aceite ISO VG 460 a 60 °C. La fabricación se ejecutó en un torno 16k20, logrando una rugosidad superficial que se ajustó a las especificaciones de diseño con un error relativo del 10 %. Los resultados técnicos son prometedores: el diseño garantiza el régimen EHL, proyectando una vida útil estimada de 1 348 000 horas. Este buje optimizado asegura la operatividad de equipos imprescindibles, mitigando costosos tiempos de inactividad en procesos clave de la cadena de valor del níquel.

Palabras clave: análisis tribológico, bronce fosforoso, cojinete de deslizamiento, lubricación elastohidrodinámica

1. INTRODUCTION

The application of sliding bearings is not limited to tools or auxiliary devices; they are fundamental components in the sector's heavy and critical machinery. These elements are vital in systems operating under extreme load and temperature conditions, finding application in: slurry pumps, ore conveyors, speed reducers, rotary dryers, ball mills, and in the alignment and support mechanisms of processing furnaces.

The unavailability of any equipment that depends on a bushing can significantly halt or delay production. Therefore, bearing reliability is a determining factor in operational continuity.

Although the sliding bearing is a widely used solution, the working environment in nickel metallurgy—characterized by high corrosion, humidity, abrasion, and dynamic loads—demands a specific and rigorous analysis. A generic design is insufficient and can lead to catastrophic failures. Consequently, the selection of materials (specific bronzes) and the optimization of the lubrication regime must strictly adhere to actual operating parameters (load, speed, temperature, and chemical environment).

These bearings ideally operate through hydrodynamic or hydrostatic lubrication, where a lubricant film separates the surfaces, offering low friction, high precision, and stability (Michalec *et al*., 2021; Harishkumar *et al*., 2023). However, their effectiveness requires high manufacturing precision and design optimization (Michalec *et al*., 2021; Wang *et al*., 2025). Wear is a common and costly cause of failure, representing a significant fraction of the total production cost (Ramírez, 2023; Jacobs and Baszenski, 2024).

The manufacture and optimized design of a specialized bushing ensure the availability of key equipment, whether main or auxiliary. The development of a specialized sliding bearing, applied to the restoration of any critical asset, resolves the unavailability of essential components for mining-metallurgical processes, fully justifying the investment in its design and manufacture.

Precise manufacturing and rigorous quality control are indispensable for critical components like bushings to meet specifications (García *et al*., 2022; Wang *et al*., 2025). A systematic approach is required, including the appropriate selection of materials and lubricants, rigorous dimensional control, and the application of validated wear models (Lehmann *et al*., 2023; García *et al*., 2023; Dimitri *et al*., 2025). Manufacturing benefits from Lean principles (Kofi *et al*., 2023; Santos, 2025), although machining advanced materials presents challenges such as tool wear and impact on surface integrity (Kumar, 2022; Prasad *et al*., 2022). Additionally, additive manufacturing (SLA) offers a solution for custom parts, but its hardness and wear properties must be evaluated (Muñoz *et al*., 2024).

In the context of critical equipment restoration, the manufacture, control, and evaluation of a replacement bushing are of vital importance (García *et al*., 2022; Wang *et al*., 2025). A well-designed bushing restores original performance, minimizes wear, and prolongs service life (Harishkumar et al., 2023; Wang *et al*., 2025). This work seeks to promote local solutions and technological self-sufficiency (García *et al*., 2024), since the quality of the sliding bearing is decisive for the long-term durability of the equipment (García *et al*., 2023; Jacobs and Baszenski, 2024).

The objective of this article is to characterize the manufacturing process, the implemented quality control, and the evaluation of a sliding bearing manufactured for the restoration of critical equipment, ensuring reliability and durability.

2. MATERIALS AND METHODS

2.1. Characteristics of the sliding bearing

The sliding bearing under study (Figure 1) is a cylindrical component manufactured from a high-performance bronze alloy, specifically selected for its superior wear resistance, surface fatigue resistance, and ability to operate under high loads. Its geometric design and rigorous control of surface finish were optimized to guarantee operation under an elastohydrodynamic lubrication (EHL) regime, maximizing reliability and significantly prolonging the equipment's service life.

Figure 1. Sliding bearing.

2.2. Measuring instruments used

The following instruments were used for the development of measurements: universal caliper with an accuracy of 0.02 mm (range 0-150 mm); TH170 portable hardness tester, measuring on the Rockwell B and C, Vickers, Brinell, Shore, and Leeb scales, with an accuracy of ± 8 %, used to measure the surface hardness of the bushing and shaft; external micrometer with an accuracy of 0.01 mm (range 0-25 mm), used to measure diameters; TR200 roughness tester, to evaluate surface roughness Ra (range 0.01 μm - 40 μm) with an accuracy of ⩽ ± 10 %; and an Spectrolab 230, to determine the chemical composition of the sliding bearing material, with relative standard deviations below 5 % for major elements and between 5 % and 10 % for trace elements.

2.3. Lathe and tools used

A 16k20 lathe was used, with a speed range from 12.5 r/min to 1,600 r/min; longitudinal feed 0.05 mm/r to 2.8 mm/r and transverse feed 0.025 mm/r to 1.4 mm/r. The specific tools were: for external turning, CCMT 09 T3 -- 04 WF 3005 insert with SCLCR/L 1212F09 -- M holder; drilling, 7 mm drill, R415.5 -- 0690 -- 30.8C0 1040; parting off, N123F2 -- 0250 -- 0001 -- CF 4025 insert with LF123F10 -- 1616B holder (Sandvik, 2000).

2.4. Operating parameters of the sliding bearing

The revolutions, load, and operating temperature were determined. The radial force (Ay) acting on the bearing (Figure 2) is calculated using equation 1, applying the equilibrium of bending moments at point B (Rodríguez, 2025).

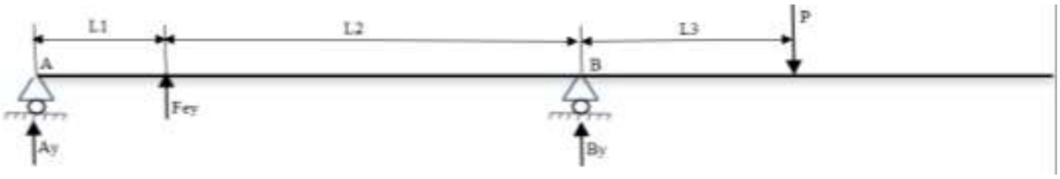

Figure 2. Diagram of the forces acting on the system (beam).

$$Ay = \frac{P \cdot L3 + Fey \cdot L2}{L1 + L2} \tag{1}$$

Where: Ay is the radial force acting on the bushing (N); P is the total weight, including the shaft, sprocket, and mandrel (N); L3, distance from point B to the center of mass (mm); Fey, radial force of the helical cylindrical transmission (N); L2, distance from the point of application of the radial force (Fey) to point B in mm; L1, distance from point A to the point of application of force Fey (mm).

The weight P is determined by multiplying the mass of the shaft, mandrel, and gear assembly by the acceleration due to gravity; L3 in AutoCAD by geometric procedure (3D horizontal drawing of the shaft, gear, and mandrel assembly, and calculation of the center of mass coordinate); Fey by multiplying the driving tangential force by the tangent of the transverse pressure angle; L1 and L2 by measurement. The radial force Fey is determined from the fundamental principles of force relationships and standard helical gear geometry (Budynas and Keith-Nisbett, 2012), as shown in the following equation 2.

$$Fey = \frac{60 \cdot Np \cdot (Z + 2 \cdot \cos(\psi))}{\pi \cdot n \cdot De \cdot Z} \cdot \frac{\tan(\propto)}{\cos(\psi)} \tag{2}$$

Where: Np is the transmitted power (W); α is the normal pressure angle (degrees); Z, number of teeth of the gear; ψ, helix angle (degrees); *n*, rotational speed (r/min); De, outside diameter of the gear wheel (m).

The precise determination of these operating parameters (load and rotational speed) is fundamental for tribological design.

The ideal operating temperature of a bearing is 50 °C, although high revolutions allow operation at higher temperatures. Elevated temperatures can reduce lubricant effectiveness, but if induced or by radiation, service is maintained by selecting an oil with appropriate viscosity (Rodríguez, 2025).

2.5. Sliding bearing design

The bearing material was identified through inspection, chemical analysis, and hardness testing, establishing that the shaft surface hardness should be in the range of 165 to 400 HB (SKF 2025). The configuration and size were based on the original bushing and SKF recommendations (2025), calculating the sliding speed and specific load, using equations 3 and 4, respectively.

$$Vd = \frac{\pi \cdot D \cdot n}{60 \cdot 1000} \quad (3)$$

Where, Vd is the sliding speed, m/s; D shaft diameter, mm.

$$Pe = \frac{Ay}{L \cdot D} \quad (4)$$

Where, Pe is the specific load acting on the bearing, N/mm²; L is the length of the bushing in mm.

The friction coefficient (f) was determined using the methodology of Dobrovolski and Mott (Leyva, 2016), with slight adaptations to the specific case of the sliding bearing under study (Rodríguez, 2025). Interface specifications followed the F7/e8 fit (SKF 2025). Diametral and radial clearance were calculated according to Leyva (2022), depending on the diameter, temperature, fit precision, and material property. Surface finish was defined using Hernández's tables (2010).

The minimum lubricant film thickness, film thickness ratio, Sommerfeld number, and friction coefficient were calculated, all based on Budynas and Keith-Nisbett (2012), Leyva (2016), and Rodríguez (2025).

2.6. Lubrication regime

The lubrication regime is defined by calculating the lubricant film thickness ratio (equation 5) and comparing it with the parameters in Table 1 (Del Castillo, 2007).

$$\lambda = \frac{ho}{(Rz1^2+Rz2^2)^{0,5}} \tag{5}$$

Where, λ is the film thickness ratio (dimensionless); h_0 is the minimum lubricant film thickness (mm); Rz_1, roughness of the hole (µm); Rz_2, roughness of the shaft (µm).

Table 1. Parameters of lubrication regimes

Lubrication Regime	**h_0 (µm)**	**(λ)**	**(f)**
Boundary	0.005 – 0.1	< 1	0.03 – 0.4
Mixed	0.01 – 1.0	1 - 3	0.02 – 0.2
Elastohydrodynamic	0.01 – 10	3 - 10	0.01 – 0.1
Hydrodynamic	1 - 100	> 6	0.001 – 0.01

The dynamic viscosity of the lubricant is determined using equation 6 (Mott, 2006). The required dynamic viscosity at the operating temperature is established using a graph based on ISO 7902-2, 1995 (Leyva, 2016).

$$\mu e = \frac{S \cdot Pe}{w \cdot \left(\frac{Dm}{2 \cdot Cr}\right)^2} \tag{6}$$

Where, µe is the effective dynamic viscosity of the lubricant MPa·s; S is the Sommerfeld number; Pe is the specific load on the sliding bearing, N/mm²; ω is the sliding angular velocity at the bearing and journal interface, rad/s; Dm is the journal diameter, mm; Cr is the radial clearance, mm.

2.7. Service life of the sliding bearing

The determination of the sliding bearing service life is carried out using equation 7 (GMBH, 2015).

$$Lh = \frac{Ka}{Pe \cdot (Vd)^{1,2}} \cdot Fp \cdot Fc \cdot Fd \cdot Fm \tag{7}$$

Where Lh is the bearing life in hours; Ka is a constant dependent on the field of application; Fp is the load correction factor; Fc is the temperature correction factor; Fd is the size correction factor; Fm is the material correction factor. The constant Ka and the correction factors are determined according to the GMBH table (2015); speed and specific load are determined through equations 3 and 4, respectively.

2.8. Bushing manufacturing regimes

The definition of the bushing manufacturing regimes, which include rotational speed, feed, depth of cut, number of passes, and machining time, is carried out applying the calculation equations proposed by Sandvik (2000).

2.9. Elaboration of measurement results

It was based on ensuring representativeness, normality, and comparison of results. This involved replicating measurements, establishing tolerance limits, and determining the relative error (Hernández, 2010; Miller and Freund, 2021).

3. RESULTS

3.1. Operating parameters of the sliding bearing

The evaluation of operational parameters (speed, load, and temperature) is essential for bearing durability.

Rotational speed: the kinematic analysis of the mechanism (electric motor and worm/helical gear reducer) determined that the shaft rotates at 2,800 r/min.

Loads: the total load on the bearing is a combination of the weight of the rotating assembly (shaft, wheel, mandrel) and the radial force of the gear (Figure 2); the assembly weight is 6.282 N (with *m* = 0.641 kg; *g* = 9.8 m/s²); and the radial force determined by equation 2 is 644.782 N (with Np = 1,000 W; Z = 38; ψ = 15°; α = 20°; *n* = 2,800 r/min; De = 0.04 m). Applying equation 1 (with L1 = 15 mm, L2 = 20 mm, L3 = 31 mm) for moment equilibrium, the total radial force on the bearing is 374.011 N.

Temperature: although 50 °C is ideal (Rodríguez, 2025), the high operating speed and ambient heat suggest a design temperature of 60 °C; this condition requires choosing a lubricant with adequate viscosity to avoid premature wear.

3.2. Analysis of the bearing design

Material characterization (Table 2) and Vulcanometals standards (Cáseres, 2019) allowed identifying the worn bushing as aluminum bronze

CuAl10Ni (163 HB with standard deviation 7.23 HB) and the new one as phosphorous tin bronze CuSn14 (232 HB with standard deviation 7.47 HB).

Table 2. Chemical composition of the bushing material

Material	Cu	Sn	Pb	Zn	Fe	Ni	Mn	Al	Si
Bronze CuAl10Ni	79	...	0.03	...	3.5 4.5	4 5	0.8 1.5	8.5 9.5	0.1
Worn bushing	78	...	0.025	...	3.2	4.4	1.1	9.2	0.08
Bronze CuSn14	86 89	12 14	0.25	0.25	0.15	0.5	...	...	...
New bushing	88	12.5	0.24	0.23	0.16	0.45	...	...	...

The hardness of the shaft (278 HB) was 1.71 times higher than that of the worn bushing and 1.2 times higher than that of the new bushing. The 42.33 % increase in hardness is the cornerstone of the recovery strategy, as it provides significantly superior wear resistance. It is confirmed that the bushing acts as a sacrificial element (SKF 2025). The geometric configuration (Figure 3) and design temperature (60 °C) were analyzed.

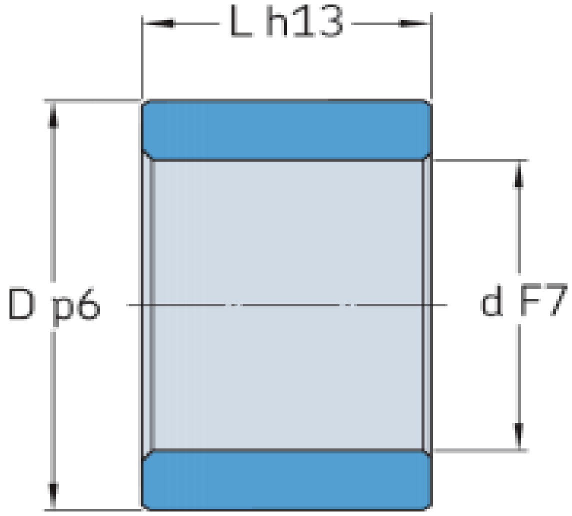

Figure 3. Tolerances for solid bronze plain friction bearings (SKF, 2025).

It was verified that the sliding speed (Vd) calculated using equation 3 is 0.00011 m/s, less than 0.01 m/s, and the specific load (Pe) calculated by equation 4 is 6.68 N/mm², less than 50 N/mm²; both values are below the limits recommended by SKF (2025). This geometric and load validation indicates that the bearing is oversized for nominal conditions, which minimizes the risk of damage or premature wear and contributes to ensuring safe performance and a long service life of the component in the industrial environment.

To determine the coefficient of friction, methodologies from Dobrovolski and Mott were applied (Rodríguez, 2025). For a radial clearance (Cr) of 0.020 mm, safety factor (k) of 2.5, and solid particle size in the lubricant (ha) of 2.5 μm, the minimum film thickness (h_0) was 0.01 mm, resulting in a Sommerfeld number (S) of 0.18 and a friction coefficient (*f*) of 0.023. Since 0.01 < *f* < 0.1, it is determined that the bearing operates (Table 1) under an elastohydrodynamic lubrication regime (Del Castillo, 2007).

3.3. Bearing lubrication

Additionally, for greater precision, the lubrication regime was determined by calculating the film thickness ratio (λ), using equation 5 and Table 1. With a minimum film thickness (h_0) of 0.01 mm and roughnesses *Rz1 = Rz2* = 0.8 μm, λ = 9.06 was obtained. This result, being in the range of 3 to 10, indicates an elastohydrodynamic lubrication regime (Del Castillo, 2007), ensuring the protection of the kinematic pair. Achieving this regime is the technical proof that the design guarantees total separation of the surfaces, which is essential for the durability and reliability of the bushing.

The required effective dynamic viscosity was determined using equation 6, considering the Sommerfeld number (S = 0.18), specific load (Pe = 6.68 N/mm²), angular velocity (ω = 293.07 rad/s), mean diameter (Dm = 7.003 mm), and radial clearance (Cr = 0.02 mm), resulting in 132 MPa·s. Considering that petroleum-derived oils should be limited to 70 °C to retard oxidation (Mott 2006), and using ISO 7902-2 (1995) for the operating temperature of 60 °C, it is concluded that the appropriate lubricant is an ISO VG 460.

The selection of this high-viscosity lubricant is a specific and preventive engineering measure to counteract the adverse effects of high speed and design temperature, ensuring that the lubricant film maintains its integrity and effectiveness in the demanding mining-metallurgical environment.

3.4. Estimation of bearing service life

The estimated service life of the bearing (Lh), in hours, was performed by applying equation 7 proposed by GMBH (2015), which incorporates specific correction factors. The factors used were: Ka = 400 (local load), Fp = 1 (since Pe = 6.68 N/mm² < 10 N/mm²), Fc = 1.6 (intermittent operation), Fd = 1 (shaft less than 20 mm), and Fm = 0.4 (bronze). Substituting these values, together with the specific radial load (Pe = 6.68 N/mm²) and sliding speed (Vd = 0.00011 m/s), an estimated service life of 1,348,000 hours was obtained.

This contributes to ensuring the long-term operational reliability of the equipment, which directly translates into reduced maintenance costs and increased availability.

3.5. Bushing manufacturing regimes

The definition of the manufacturing regimes was crucial to transfer the design specifications (material and surface finish) to the production reality, despite the limitations of the available machinery.

The determination of the manufacturing regimes was based on the analysis of the phosphor bronze bushing (CuSn14) design, the required dimensions according to the worn bushing, and SKF recommendations (2025), detailed in Figure 4. The manufacturing process is carried out on a 16k20 lathe from a semi-finished product 30 mm long by 20 mm in diameter, and includes sequential operations of facing, turning, drilling, and parting off.

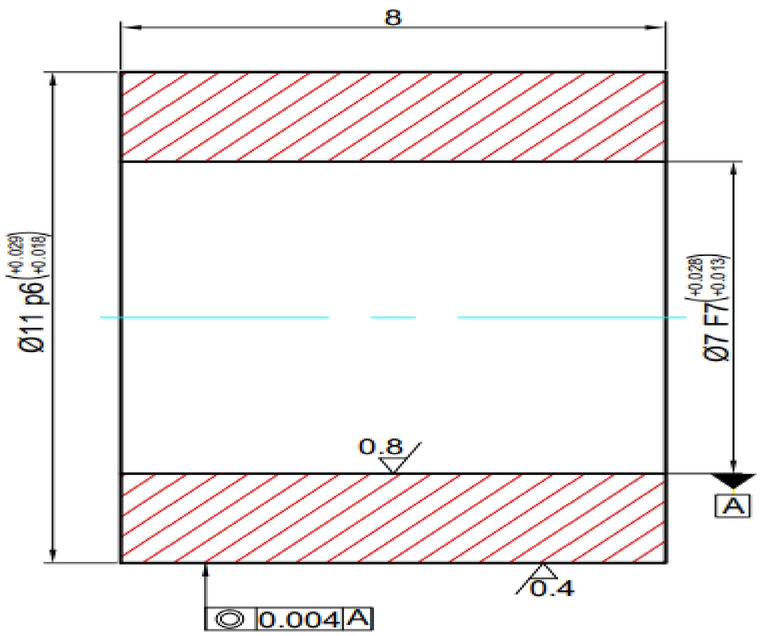

Figure 4. Sketch of the sliding bearing.

The cutting speed (Vc), calculated according to Sandvik (2000), revealed a limitation: the maximum speed of the 16k20 lathe (1,600 r/min) prevents reaching the recommended minimum Vc (e.g., 240 m/min, adjusted by Kv = 1.09 for the CCMT 09 T3 -- 04 WF 3005 insert). This restriction causes underutilization of the tools in all operations, including drilling (R415.5

-- 0690 -- 30.8C0 1040 drill) and parting off (N123F2 -- 0250 -- 0001 -- CF 4025 insert). To compensate for the low cutting speed and ensure the surface finish, a compensation strategy was implemented: the feed (fn) was selected at the machine's minimum (0.025 mm/r for facing/parting; 0.05 mm/r for drilling/turning), based on the machine specifications and manufacturer's tables (Sandvik, 2000). The depth of cut (*t*) was set at 3 mm, requiring one pass for facing and two passes for turning.

The machining time (Tm), calculated using Sandvik's equation (2000), totaled 1.125 min (facing: 0.4 min; turning: 0.35 min; drilling: 0.175 min; parting: 0.2 min). Although the total time is short, the underutilization of tools due to the speed limitations of the 16k20 lathe suggests that selecting equipment with higher capacity would optimize process efficiency; however, at the time of manufacturing the sliding bearing, no other lathe was available.

This manufacturing process, based on the part drawing and described in the technological chart (Rodríguez 2025), is proof of engineering's ability to solve the shortage of spare parts by adapting existing resources, a key factor for technological self-sufficiency in the mining-metallurgical industry.

3.6. Control of the bushing construction parameters

Quality control is the stage that links theoretical design with practical functionality, ensuring that the manufactured bearing meets the critical dimensional and surface specifications required to operate under the EHL lubrication regime.

Quality control focused on verifying the dimensions and surface properties of the bushing to ensure correspondence with the design specifications. For surface finish, a process control chart was used based on surface roughness (Ra) measurements, as illustrated in Figure 5, LST(R) and LIT(R) are the tolerance limits determined according to Hernández (2010); Miller and Freund (2021). This chart, with a 95 % confidence level, confirmed that the process remained under statistical control.

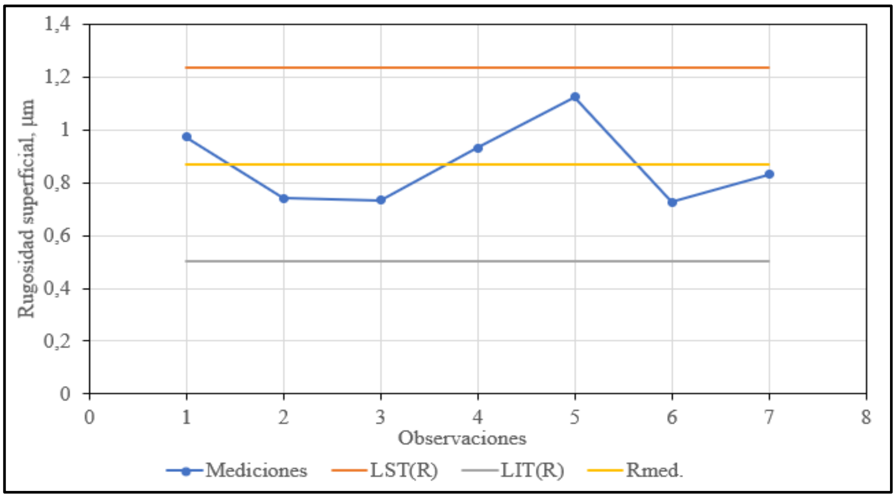

Figure 5. Control chart for surface roughness measurements in Ra.

The average roughness obtained on the inner surface of the bushing was 0.88 µm. To compare this value with the roughness specified in the design (0.8 µm), a relative error of 10 % was calculated. This result is fundamental, as it validates the compensatory machining strategy applied given the limitations of the 16k20 lathe. A low relative error guarantees the quality of the surface finish required for the proper development of the lubricant film.

Confirmation that the surface roughness conforms to the design is crucial for the effective activation of the elastohydrodynamic lubrication regime. This control of construction parameters ensures that the bushing not only has the correct hardness and material but also the necessary surface finish to guarantee the high durability and reliability of the equipment in the mining-metallurgical industry. Additionally, it was verified that the inner and outer diameters, together with the bushing length, complied with the established dimensional limits.

4. CONCLUSIONS

- The study of the design, manufacture, and evaluation of the sliding bearing allows the effective recovery of equipment for the continuity of processes in the nickel mining-metallurgical industry.
- It is identified that the worn bushing was composed of aluminum bronze (CuAl10Ni), while the replacement bushing was manufactured with phosphorous tin bronze (CuSn14). The average hardness of the new sliding bearing (232 HB) is 42.33 % higher than that of the worn component (163 HB), which confers greater wear resistance.

- The selection of ISO VG 460 lubricant for a design temperature of 60 °C, radial load of 374.011 N, and rotational speed of 2,800 r/min in the bearing is crucial for maintaining the hydrodynamic film, which translates into an estimated service life of 1,348,000 hours.
- The surface roughness obtained on the inner surface of the bushing conforms to the design specification with a relative error of only 10 %, demonstrating the capacity of local engineering to solve the shortage of spare parts and maintain the operability of critical equipment in the mining-metallurgical sector.

5. REFERENCES

Budynas, R. C. y Keith-Nisbut, J. (2012). *Diseño en ingeniería mecánica.* 9na edición. New York: McGraw-Hill, 1029 p. http://www1.frm.utn.edu.ar.

Carrión, A. G.; Aldas, D.; Lascano, N. y Ayala, M. (2024). La sostenibilidad ambiental en la industria manufacturera del Ecuador. Un estudio desde las fuentes energéticas. *Revista Ciencia UNEMI, 17*(44), 148-161. https://doi.org/10.29076/issn.25287737vol17iss44.2024pp148-161p.

Cáseres, A. A. (2019). *Cobre - Bronce, latón - babbitt.* Vulcanometals, Lima, 24 p. Consultado 23 de junio de 2025, en: wwwvulcanometals.com.

Del Castillo, F. D. (2007). *Tribología: fricción, desgaste y lubricación*. Izcalli, Cuautitlán, 25 p. http://profefelipe.next.

Dimitri, A. S.; Rashed, N. A.; Hegazi, H. A. and EL-Shazly, M. H. (2025). Design optimization of multipoles radial magnetic bearings for large industrial rotors. *Journal of Engineering and Applied Science*, *72*(108), 2-8. https://doi.org/10.1186/s44147-025-00678-w.

García, A.; Echevarría, D.; Triana, J. A.; Triana, J. P.; Cruz, K. y González, R. (2024). Reporte sobre economía cubana enero-julio 2024. Centro de estudio de economía cubana. https://library.fes.de.

García, A. E.; González, G.; Aguilera, C. D; De la Torre, F. y Abreu, O. (2022). Evaluación de cojinetes de deslizamiento basada en la norma ISO 7902:2020. *Revista Ingeniería Mecánica, 25*(2), 1-8. https://www.ingenieriamecanica.cujae.edu.cu.

García, A. E.; Penabad, L.; Aguilera, C. D.; Barrera, C. y Guillén, J. (2023). Modelo para la gestión de la lubricación y los lubricantes en la industria. *Ingeniería Mecánica, 26*(3), 1-9. http://www.ingenieriamecanica.cujae.edu.cu.

Harishkumar, K.; Chandrakant, R. and Satish, Sh. (2023). Effect of Cavitation and Temperature on Fluid Film Bearing Using CFD and FSI Technique: A Review. *Archives of Computational Methods in Engineering, 30*, 1623–1636. https://doi.org/10.1007/s11831-022-09847-z.

Hernández, F. D. (2010). *Metrología dimensional*. 2da edición. Ciudad Habana: Félix Varela, 507 p. https://isbncuba.ccl.cerlalc.org.

Jacobs, G. and Baszenski, Th. (2024). Detection of wear in sliding bearings with the use of machine learning techniques. *Tribologie und Schmierungstechnik,* 18-28. DOI: 10.24053/TuS-2023-0036.

Kofi, R.; Yeboah, E.; Yeboah, E.; Agyapong, G. and Efua, S. (2023). Sustainable manufacturing practices and sustainable performance: Evidence from Ghana's food manufacturing sector. *Cleaner Logistics and Supply Chain, 9*, 1-15. https://doi.org/10.1016/j.clscn.2023.100120.

Kumar, R. (2022). Effect of tool wear on surface roughness in machining of AA7075/ 10 wt.% SiC composite. *Composites Part C: Open Access,* 1-19. http://www.sciencedirect.com/journal/composites-part-c-open-access.

Lehmann, B.; Trompetter, P.; Gutiérrez, F. and Jacobs, G. (2023). Evaluation of Wear Models for the Wear Calculation of Journal Bearings for Planetary Gears in Wind Turbines. *Revista lubricants, 11*(364), 1-18. https://doi.org/10.3390/lubricants11090364.

Leyva, B. (2022). *Guía para clases prácticas de mediciones técnicas: Orientaciones y sistemas de ejercicios.* Editorial Académica Española, 104 p. https://www.amazon.ie.

Leyva, A. (2016). *Análisis de cojinetes radiales de contacto deslizante de los ventiladores de tiro forzado de la termoeléctrica Lidio Ramón Pérez.* Amaury Gilbert Hernández e Isnel Rodríguez González (Tutores). (Tesis de ingeniería mecánica, Instituto Superior Minero Metalúrgico de Moa). 77 p. https: ninive.ismm.edu.cu.

Michalec, M.; Svoboda, P.; Krupka, I. and Hartl, M. (2021). A review of the design and optimization of large-scale hydrostatic bearing systems. *Revista Engineering Science and Technology, an International Journal, 936-958.* https://doi.org/10.1016/j.jestch.2021.01.010.

Miller, I. y Freund, J. E. (2021): *Probabilidad y estadística para ingeniero.* 4ta edición. Editorial Reverté, Barcelona, 403 p. https://api.pageplace.de.

Mott, R. L. (2006). *Diseño de elementos de máquinas.* 4ta edición. Ciudad de México: Pearson Educación, 628 p. https://www.udocz.com.

Muñoz, P.; Villena, O.; Mayorga, L.; Pérez, D. y Moya, D. (2024). Predicción de desgaste abrasivo y dureza superficial de partes impresas por tecnología SLA. *Revista Ingenius, 31*, 19-38. https://doi.org/10.17163/ings.n31.2024.02.

Prasad, A., Kumar, A. and Gajrani, K. (2022). *Advances in Sustainable Machining and Manufacturing Processes.* Editorial Taylor y Francis Group. ISBN: 978-1-032-08165-6. DOI: 10.1201/9781003284574.

Ramírez, F. (2023). Modelos de desgaste de herramientas: Sobre la hipótesis de modelización. *Ingeniare. Revista Chilena de Ingeniería*, *31*(9), 1-14. https://orcid.org/0000-0002-2156-7263.

Rising, J. A.; Taylor, Ch., Ives, M. C. and Ward, R. (2022). Challenges and innovations in the economic evaluation of the risks of climate change. *Ecological Economics, 197*, 1-13. http://www.elsevier.com/locate/ecolecon.

Rodríguez, C. M. (2025). *Evaluación y construcción de un cojinete de deslizamiento para taladro portátil ID13-HYL1135.* Benigno Leyva De la cruz y Eli Efraín Guzmán Romero (Tutores). (Tesis de grado, Universidad de Moa). 71 p. https: ninive.ismm.edu.cu.

Sandvik. (2000). *Torneado, fresado y taladrado*. 6ta edición. Suecia: Sandvik Coromant, 217 p. www.coromant.sandvik.com.

Santos, B. L. (2025). Cadenas de suministro sostenibles en la industria manufacturera: innovación, conocimiento y gestión lean. *Revista de Estudios Interdisciplinarios en Ciencias Sociales, 27*(3), 867-876. www.doi.org/10.36390/telos273.07.

SKF. (2025). Diseño y versiones de cojinetes de deslizamiento SKF. Consultado: 14/06/2025. Disponible en: https://www.skf.com/ar/products/plain-bearings/bushings-thrust-washers-strinps/bushings/desingns-variants.

TTV, GmbH. (2015). Cojinetes deslizantes - información técnica. Consultado: 18/06/2025. Disponible en: https://www.ttvgmbh.de/pdf/Gleitlager/Technische-Infos.

Wang, L.; Han, J.; Tang, Z.; Zhang, Y., Wang, Y. and Li, X. (2025). Geometric Accuracy Design of High-Performance CNC Machine Tools: Modeling, Analysis, and Optimization. *Chinese Journal of Mechanical Engineering, 38*(87), 2-35. https://doi.org/10.1186/s10033-025-01258-y.

Additional information

Conflict of interest

The authors declare that there are no conflicts of interest.

Author contributions

BLDC: research design, performing measurements, processing and interpretation of results, original manuscript writing, correction, and approval of the final report. EEGR: research design, review of the original manuscript, analysis of results, approval of the final report. MFSC: bibliographic and results analysis, review and approval of the final report. HLLA: literature review, analysis of results, review and approval of the final report. WGQS: literature search, methodology, analysis of results, and approval of the final report. YRM: research design, bibliographic management, preparation and review of the original manuscript, analysis of results, correction, and approval of the final report.

ORCID

BLDC, https://orcid.org/0009-0004-9080-1406
EEGR, https://orcid.org/0000-0003-4906-8009
MFSC, https://orcid.org/0000-0003-1785-1568
HLLA, https://orcid.org/0000-0003-2688-015X
WGQS, https://orcid.org/0000-0001-9430-2082
YRM, https://orcid.org/0000-0002-5098-5675

Received: 10/30/2025
Accepted: 11/15/2025